

Cite this: *RSC Med. Chem.*, 2021, 12, 1164

Optimization of brain-penetrant picolinamide derived leucine-rich repeat kinase 2 (LRRK2) inhibitors†

Anmol Gulati,^a Charles S. Yeung,^a Blair Lapointe,^a Solomon D. Kattar,^a Hakan Gunaydin,[‡] Jack D. Scott,^b Kaleen K. Childers,[§] Joey L. Methot,^a Vladimir Simov,^a Ravi Kurukulasuriya,[‡] Barbara Pio,^b Greg J. Morriello,^b Ping Liu,^b Haiqun Tang,^b Santhosh Neelamkavil,[¶] Harold B. Wood,^b Vanessa L. Rada,^c Michael J. Ardolino,^a Xin Cindy Yan,^a Rachel Palte,^a Karin Otte,^a Robert Faltus,^a Janice Woodhouse,^a Laxminarayan G. Hegde,^a Paul Ciaccio,^a Ellen C. Minnihan,^{||} Erin F. DiMauro,^a Matthew J. Fell,^a Peter H. Fuller^a and J. Michael Ellis^{**a}

The discovery of potent, kinome selective, brain penetrant LRRK2 inhibitors is the focus of extensive research seeking new, disease-modifying treatments for Parkinson's disease (PD). Herein, we describe the discovery and evolution of a picolinamide-derived lead series. Our initial optimization efforts aimed at improving the potency and CLK2 off-target selectivity of compound **1** by modifying the heteroaryl C–H hinge and linker regions. This resulted in compound **12** which advanced deep into our research operating plan (ROP) before heteroaryl aniline metabolite **14** was characterized as Ames mutagenic, halting its progression. Strategic modifications to our ROP were made to enable early de-risking of putative aniline metabolites or hydrolysis products for mutagenicity in Ames. This led to the discovery of 3,5-diaminopyridine **15** and 4,6-diaminopyrimidine **16** as low risk for mutagenicity (defined by a 3-strain Ames negative result). Analysis of key matched molecular pairs **17** and **18** led to the prioritization of the 3,5-diaminopyridine sub-series for further optimization due to enhanced rodent brain penetration. These efforts culminated in the discovery of ethyl trifluoromethyl pyrazole **23** with excellent LRRK2 potency and expanded selectivity *versus* off-target CLK2.

Received 18th March 2021,
Accepted 6th May 2021

DOI: 10.1039/d1md00097g

rsc.li/medchem

Introduction

Parkinson's disease (PD) is a chronic, progressive neurodegenerative disorder that afflicts over 10 million people worldwide and is the second most common neurodegenerative disorder after Alzheimer's disease (AD).

^a Merck & Co., Inc., 33 Avenue Louis Pasteur, Boston, Massachusetts 02115, USA.

E-mail: anmol.gulati@merck.com, charles.yeung@merck.com;

Tel: +1 617 992 2472, +1 617 992 3113

^b Merck & Co., Inc., 2015 Galloping Hill Road, Kenilworth, New Jersey 07033, USA

^c Merck & Co., Inc., 770 Sunnyside Pike, West Point, Pennsylvania 19486, USA

† Electronic supplementary information (ESI) available. See DOI: 10.1039/d1md00097g

‡ Current address: Relay Therapeutics, 399 Binney St, Cambridge, Massachusetts 02139, USA.

§ Current address: Moderna, 200 Technology Square, Cambridge, Massachusetts 02139, USA.

¶ Current address: The Janssen Pharmaceutical Companies of Johnson & Johnson, 3470 Broadway, New York, New York 10031, USA.

|| Current address: Bill & Melinda Gates Medical Research Institute, Cambridge, Massachusetts 02141, USA.

** Current address: Bristol Myers Squibb, 200 Cambridge Park Drive, Suite 3000, Cambridge, Massachusetts, 02140, USA.

Age is the most significant risk factor for the onset of PD, and disease prevalence is expected to increase in the future. Characteristic motor symptoms of PD include foot and hand tremors, followed by bradykinesia, muscle rigidity, and postural instability. On a neuropathological level, these symptoms are caused by the progressive loss of dopaminergic neurons in the substantia nigra.^{1,2} FDA approved therapies for PD, *e.g.* levodopa, dopamine agonists, and monoamine oxidase-B inhibitors, are intended to manage a patient's symptoms, however, these treatments are often associated with adverse events including nausea, impulsive or compulsive behaviors, and hallucinations. Currently, there

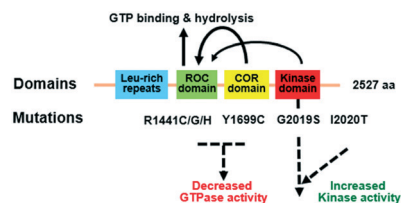


Fig. 1 LRRK2 structure. Figure adapted from Wallings *et al.* (2015).¹⁴

are no disease-modifying therapies that slow or stop the progression of this devastating neurodegenerative disorder.

Leucine-rich repeat kinase 2 (LRRK2), is a large, multidomain containing protein that in humans is encoded by the PARK8 gene (Fig. 1).^{3–5} Autosomal dominant mutations in the LRRK2 gene are the most common cause of monogenic PD and account for approximately 4–5% of familial and 1–2% of sporadic PD cases.^{6,7} The glycine 2019 to serine mutation (G2019S) is the most common of the seven pathogenic, dominantly inherited missense mutations. The G2019S and I2020T mutations reside within the kinase domain and confer an approximately 2 to 4-fold increase in kinase activity presumably through a destabilization of an inhibited form of wild-type LRRK2.^{8,9} The R1441G/C/H mutations within the ROC-COR GTPase domain enhance GTP binding, increasing kinase activity.¹⁰ Finally, the G2385R mutation within the WD40 domain disrupts dimerization resulting in a moderate increase in kinase activity through an unknown mechanism.¹¹ Independent of these well-characterized pathogenic mutations, increased kinase activity has been observed in the post-mortem brain tissue of idiopathic (“WT LRRK2”) PD patients.¹² Taken together, these data support a hypothesis that central inhibition of LRRK2 kinase activity may modify the progression of Parkinson's disease.¹³

Protein kinases represent a tractable, clinically validated drug class with over 40 inhibitors approved by the FDA and many more undergoing clinical trials.¹⁵ Advances in achieving the requisite potency to compete with millimolar ATP concentrations in cells and selective protein kinase inhibition have contributed to the success of kinase inhibitor drug development and fuel efforts to expand their clinical benefit beyond oncology. The pursuit of brain penetrant LRRK2 inhibitors for the treatment of Parkinson's disease requires enhanced levels of kinase off-target selectivity be achieved while designing within the confines of CNS drug-like space.¹⁶ Indeed, thorough analyses of the disparate physicochemical properties of kinase inhibitors and CNS drugs have been reported by Heffron¹⁷ and Mader,¹⁸ and key parameters such as hydrogen-bond donor (HBD) count, topological polar surface area (tPSA), molecular weight (MW), and lipophilicity (AlogP98) must be carefully considered in the design phase to minimize CNS efflux transporter susceptibility (P-glycoprotein (P-gp) and breast cancer resistance protein (BCRP)) and maximize CNS penetration. Herein, we describe our efforts toward the optimization of a series of CNS penetrant picolinamide derived LRRK2 inhibitors that culminated in the discovery of lead compound 23 with decreased Ames mutagenicity risk and improved selectivity *versus* the off-target CLK2.

Evolution of LRRK2 inhibitors: from thiazole carboxamides to picolinamides

Through a high-throughput screen (HTS) of the Merck sample collection against recombinant wild-type LRRK2

enzyme, we identified thiazole-4-carboxamides as a promising lead series of LRRK2 inhibitors, exemplified by 1 (Table 1). This compound possessed good on-target potency in our LRRK2 G2019S biochemical assay with physicochemical properties commensurate with CNS drugs (MW < 400, tPSA = 78, HBD = 1).^{17,18} Upon expanded profiling, we observed poor kinome selectivity as demonstrated by the 10-fold window to CDC-like kinase 2 (CLK2).¹⁹ Since CLK2 is involved in cell cycle regulation, it was deemed a potential safety liability²⁰ to advance compounds that simultaneously inhibit both LRRK2 and CLK2. As such, we incorporated a CLK2 counter-screening assay in our research operating plan (ROP) to study how the structure activity relationships (SAR) might differ between LRRK2 and CLK2. To drive expanded selectivity against CLK2 we performed docking studies of 1 in a known LRRK2 homology model.²¹ As depicted in Fig. 2, the C–H bond on the central aromatic ring (thiazole) and adjacent carbonyl (C=O) group form a H-bond donor/acceptor pair that interacts with the hinge of the kinase. Additionally, a key interaction takes place between the pyrazole nitrogen of the *N*-methylpyrazole, a putative H-bond acceptor, and catalytic lysine. We reasoned that perturbation of these motifs would impact on-target potency and CLK2 off-target selectivity. To this end, we synthesized compounds 2–4 featuring alternative 6-membered aromatic core replacements (Table 1). While *ortho*-fluorophenyl amide 2 displayed no meaningful improvements in CLK2 selectivity, we were pleased to see that pyrimidine 3 and pyridine 4 analogs offered selectivity enhancements over CLK2 (>100×). These observations may be due to a modified trajectory between the picolinamide H-bond donor/acceptor pair and the hinge binder, and an altered trajectory of the pyrazole into the catalytic lysine region (Fig. 3). Although compound 3 offered greater CLK2 selectivity compared to 4, presumably due to unfavorable interactions between the extra nitrogen in the pyrimidine ring and the lipophilic phenylalanine gatekeeper residue in CLK2 (*cf.* methionine in LRRK2), it had poor pharmacokinetics in rat (Clp > Qh). Also, 4 had decreased polarity (tPSA = 78) relative to 3 which offered greater opportunities to design in what has been characterized as a narrow physicochemical property space to navigate.^{17,18} As such, we prioritized our optimization efforts around compound 3. Indeed, related amides, GSK2578215A²² and BMPPB-32,²³ were previously characterized as potent and kinome selective LRRK2 inhibitors (*vide infra*).

Discovery of compound 12

Based on the aforementioned homology model,²⁴ the *N*-cyclobutylpyrazole of 4 projects into the solvent exposed region of LRRK2. As such, a systematic exploration of the linker was further pursued to further enhance LRRK2 potency while maintaining off-target kinase selectivity. Our previous work on *in vivo* active tool molecule MLi2 (ref. 25) led us to hypothesize that we could replace the *N*-cyclobutylpyrazole of

Table 1 Evolution of kinase hinge binders leading to the discovery of **4**. LRRK2 IC₅₀ and Cell_u IC₅₀ values reported are *n* = 1 unless other reported (see ESI† for more information). CLK2 IC₅₀ values reported are *n* = 1

	1	2	3	4
MW, tPSA, AlogP98	328, 78, 1.58	339, 65, 2.58	323, 91, 1.13	322, 78, 2.08
LRRK2 IC ₅₀ (LBE)	14 (0.47)	70 (0.39)	34 (0.43)	53 (0.41)
Cell _u IC ₅₀ (nM)	271	1647	953	905
CLK2 IC ₅₀ (nM)	119	716	17 170	5957
CLK2/LRRK2 selectivity	8.5×	10×	505×	112×

4 with a 2,4-diaminopyridine to enhance LRRK2 potency. In our design, we maintained at least one *ortho*-C–H bond on the linker aromatic ring to ensure a favorable planar geometry stabilized by intramolecular hydrogen bonding with the neighboring amide carbonyl (C=O), and installed the *cis*-2,6-dimethylmorpholine at the 2 position (Table 2). Compound **5** demonstrated a significant improvement in unbound cellular potency (38-fold) relative to **4**, however, this was accompanied by a decrease in CLK2 selectivity. Replacement of the methyl group in the ribose pocket with the larger, electron-withdrawing trifluoromethyl (CF₃) substituent (**6**) resulted in further improved unbound cellular potency (12-fold), but this also came at the expense of CLK2 selectivity. At this stage, we recognized that the selectivity gains made by replacing the hinge aryl group were diminished by the addition of the 2,4-diaminopyridine motif. However, the exceptional gains in unbound cellular potency prompted us to explore CLK2 structure activity relationships in other vectors of the scaffold.

This work began with a solvent front scan to probe the tractability of CLK2 selectivity in this region (Table 3). Toward that end, methoxy azetidines **7** maintained LRRK2 potency but did not improve CLK2 selectivity. Azetidines alcohols **8** and **9** yielded similar profiles, and we were pleased to observe that they were not P-gp substrates in our *in vitro* rat LLC-Mdr1a P-gp efflux transporter assay despite the additional HBD and increased tPSA. Pyrrolidine secondary alcohol **10** retained LRRK2 potency and slightly improved CLK2 selectivity (3×) but suffered from a poor rat pharmacokinetic profile (Cl_p = 112 mL min⁻¹ kg⁻¹, MRT = 0.5 h). To address the *in vivo* instability, the pyrrolidine was substituted at the presumed metabolic hot spots affording bridged pyrrolidine tertiary alcohol **11**. Indeed, a significant improvement in rat pharmacokinetic profile was observed while maintaining a low P-gp efflux ratio (0.8). However, **11** was unselective against CLK2. Removal of the bridge on the pyrrolidine afforded compound **12** which gratifyingly, improved CLK2 selectivity (63×), and maintained excellent unbound cellular potency and *in vivo* stability (MRT = 5.2 h). Alternative

saturated N-heterocycles were evaluated *e.g.* piperazine oxetane **13**, but inferior CLK2 selectivity was observed. This led to the prioritization of **12** for further evaluation.

Compound **12** was advanced through a battery of pharmacokinetic and safety studies. It had moderate hERG activity (hERG IC₅₀ = 7.6 μM), and weak sodium (Na⁺), and calcium (Ca²⁺) ion channel activity (Na⁺ IC₅₀ = 29.9 μM, Ca²⁺ IC₅₀ = 21.8 μM). Evaluation of **12** in a 268 protein kinase counterscreen panel revealed MINK1, CLK2, and IRAK4 as the only kinases less than 100-fold selective against LRRK2. Compound **12** was evaluated in a broad Eurofins off-target panel, and >50% inhibition was observed at 10 μM against adenosine A₁ receptor, adenosine A_{2A} receptor, tachykinin NK1, and at 1 μM against the adenosine transporter (see ESI† for details). Similar to rat, acceptable pharmacokinetics in dog was achieved as demonstrated by good MRT and % F (Table 4). Since human dose prediction is multiparametric, we sought a resource sparing “early human dose prediction” to enable effective molecule prioritization early in our design-make-test cycle.^{26,27} In our application, we defined the minimal data set to support this calculation as unbound cellular IC₅₀ (as a surrogate for target engagement) and rat *in vivo* PK. Human pharmacokinetic parameters were predicted by allometric scaling of rat clearance (rCl_p) and rat volume of distribution (V_d) to human clearance (hCl_p) and

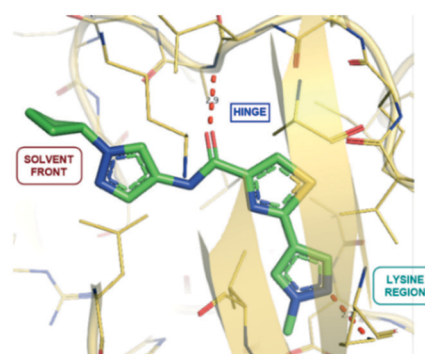


Fig. 2 Docking pose of **1** in a LRRK2 homology model.²¹

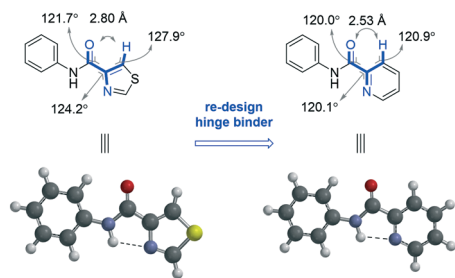


Fig. 3 Comparison of a thiazole and pyridine hinge binder. Calculations performed in Spartan using molecular mechanics (PM3).

human volume of distribution (hV_d), respectively. The rat fraction unbound (rF_u) was used as a surrogate for human fraction unbound (hF_u).^{26,27} Predicted human pharmacokinetic parameters were used to estimate the dose needed to cover the unbound IC_{50} at 12 or 24 h for BID or QD dosing, respectively. Using this methodology translated into an early human dose prediction of 178–613 mg BID for **12**.

Next, we evaluated the CNS properties of compound **12**. Unfortunately, it repeatedly failed the *in vitro* 1 μ M rat LLC-Mdr1a P-gp efflux transporter assay due to low mass balance and post-dose concentration. In the 0.1 μ M rat LLC-Mdr1a P-gp efflux transporter assay, compound **12** was characterized as a moderate P-gp substrate (rat 0.1 μ M P-gp BA/AB = 3.5, see Table 3). We then conducted an *in vivo* rat PK/PD experiment to assess its ability to inhibit the phosphorylation of LRRK2 serine 935 (pSer935) and to penetrate the CNS in rodent. Compound **12** demonstrated a dose-dependent reduction of pSer935 in rat striatum (*in vivo* rat brain unbound IC_{50} = 14 nM), and achieved a $K_{p,u,u}$ = 0.6 (Fig. 4). In the same study, control compound MLi2 performed as previously reported (72% reduction at 10 mg kg^{-1} , $K_{p,u,u}$ = 0.5).²⁵

The preclinical safety and toxicokinetic profile of **12** was examined in a 4 day tolerability study. The compound was administered orally to male rats at 50 mg kg^{-1} and 100 mg kg^{-1} BID. The compound was tolerated with no clinical signs exhibited at either dose. In the same study, **12** was found to be negative for micronucleus (MN) induction in bone marrow.

Ames mutagenicity of amino-heterocycle metabolites

Given the promising profile of **12** and cognizant of the aryl amide motif, we investigated the potential for Ames mutagenicity risk. Indeed, *in vitro* MetID suggested heteroaryl aniline **14** was formed in rat and human hepatocytes upon incubation of **12** for 120 min. Both **12** and **14** were tested in a 3-strain (TA1535, TA98, and TA100) bacterial reverse mutation (Ames) assay with S9 metabolic activation. While the parent molecule (**12**) was Ames negative, aniline metabolite **14** was Ames positive. This data led to the discontinuation of

Table 2 Summary of **5** and **6**. LRRK2 IC_{50} and Cell_u IC_{50} values reported are $n = 1$ unless other reported (see ESI† for more information). CLK2 IC_{50} values reported are $n = 1$

	5	6
MW, tPSA, AlogP98	406, 85, 2.97	460, 85, 3.40
LRRK2 IC_{50} (LBE)	9 (0.37)	4 (0.35)
Cell _u IC_{50} (nM)	24	1.5
CLK2 IC_{50} (nM)	124	21
CLK2/LRRK2 selectivity	14×	5×

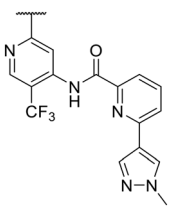
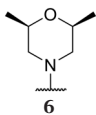
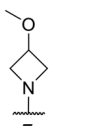
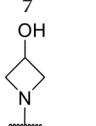
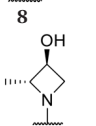
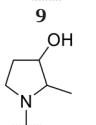
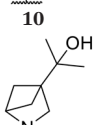
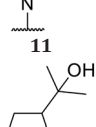
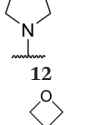
compound **12**, and a reassessment of our strategy to optimize this chemical series.

To identify alternative leads (and their corresponding aniline metabolites) de-risked for Ames mutagenicity, we employed three-strain Ames assessment early in our ROP to support SAR development. Previously, it was postulated that one mechanism through which anilines (*e.g.* **14**) exert their Ames mutagenic effect involves activation through *N*-oxidation by cytochrome P450s to form an *N*-hydroxyaniline which undergoes N–O bond cleavage to form a reactive nitrenium ion.²⁶ Presumably, this intermediate forms a covalent adduct with DNA which leads to miscoding errors during DNA replication. Hence, the stability and electronic character of the nitrenium ion is expected to impact the aniline's potential to exert Ames mutagenic effects (Fig. 5).²⁸

Next, we assessed the Ames mutagenicity risk of two electronically differentiated heteroaryl anilines, 3,5-diaminopyridine **15** and 4,6-diaminopyrimidine **16**, based on an assumption that their parent molecules would represent a reasonable starting point for further optimization. Each aniline was evaluated in the *in silico* models, MCASE and QM,²⁸ as well as the 3-strain Ames assay. While the *in silico* analysis of aniline **14** was inconclusive, *i.e.*, MCASE was negative and QM was positive (Table 5), both **15** and **16** were negative in Ames, and MCASE and QM accurately predicted these results.

Compounds **17** and **18** (derived from anilines **15** and **16**) were further characterized. Methyl pyrimidine **17** afforded inferior potency and comparable CLK2 selectivity (relative to **12**) and demonstrated good *in vivo* pharmacokinetics in rat and dog (Table 6). Evaluation in an *in vitro* rat LLC-Mdr1a P-gp efflux transporter assay revealed that **17** is a substrate for P-gp. This is likely driven by the high tPSA and presence of two hydrogen bond donors.¹⁸ Consistent with this finding, **17** demonstrated low brain penetration in a rat oral PK study ($K_{p,u,u}$ = 0.1). 3,5-Diaminopyridine **18** exhibited a slight improvement in LRRK2 potency and inferior CLK2 selectivity (relative to **17**) and

Table 3 Solvent front SAR optimization leading to the discovery of **12**. LRRK2 IC₅₀ and Cell_u IC₅₀ values reported are *n* = 1 unless other reported (see ESI† for more information). CLK2 IC₅₀ values reported are *n* = 1

	MW, tPSA, AlogP98	LRRK2 IC ₅₀ (LBE), Cell _u IC ₅₀ (nM)	CLK2 IC ₅₀ (nM)	CLK2/LRRK2 selectivity	1 μM rat LLC Mdr1a ER (B - A/A - B), Papp (10 ⁻⁶ cm s ⁻¹)	r-PK Clp mL min ⁻¹ kg ⁻¹ (Cl _{int}), MRT (h)
	460, 85, 3.4	4 (0.35), 1.5	21	5×	—	37.9 (6920), 2.7 h
	432, 85, 2.7	28 (0.33), 2.8	67	2.4×	0.46, 25	—
	418, 96, 2.3	4.8 (0.38), 7.5	64	13×	1.5, 38	—
	432, 96, 2.7	2 (0.38), 2	12	6×	1.6, 32	70 (73 016), 0.7 h
	446, 96, 2.7	5 (0.35), 3	86	17×	0.6, 29	112 (—), 0.5 h
	486, 96, 2.7	9(0.31), 2	9.6	1×	0.8, 21	24.8 (11 214), 4.4 h
	474, 96, 3.12	1 (0.36), 2.5	63	63×	3.5, 35 (0.1 μM rat LLC Mdr1a ER) (B - A/A - B), Papp (10 ⁻⁶ cm s ⁻¹)	10 (5722), 5.2 h
	501, 88, 1.5	1.5 (0.34), —	8	5×	—	2.7 (4081), 2.2 h

demonstrated good pharmacokinetics across species. Examination of **18** in the rat P-gp efflux transporter assay revealed the compound was not a substrate of P-gp, and this

translated to improved brain penetration in rat ($K_{p,u,u} = 0.4$). For this reason, we prioritized compound **18** for further optimization of on-target potency and CLK2 selectivity.

Table 4 Pharmacokinetic properties of **12**

Rat PK			Dog PK		
Cl _p mL min ⁻¹ kg ⁻¹ (Cl _{int})	MRT	% F	Cl _p mL min ⁻¹ kg ⁻¹ (Cl _{int})	MRT	% F
10 (5722)	5.2 h	16%	15 (14 531)	3.6 h	43%

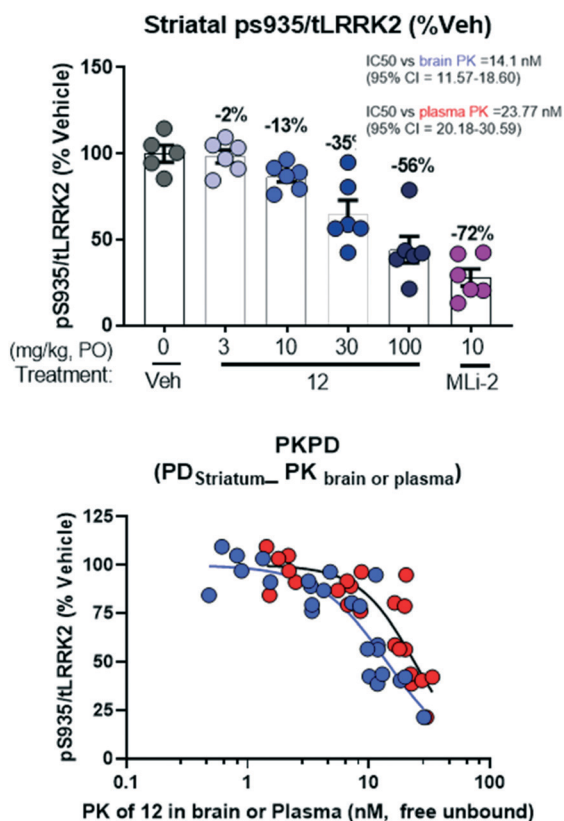


Fig. 4 Striatal PD vs. either brain or plasma PK for PK/PD analysis. IC₅₀ vs. brain PK = 14.1 nM (95% CI = 11.6–18.6). IC₅₀ vs. plasma PK = 23.8 nM (95% CI = 20.2–30.6). K_{p,u,u} = 0.6.

To enable our designs, an X-ray structure of the recently disclosed CHK1-LRRK2 chimera²³ with **18** (PDB code: 7MCK) was obtained. An overlay of compound **18** and BMBPB-32 (PDB code: 5OP2),²³ a potent and kinome selective benzamide LRRK2 inhibitor, was generated to understand and compare the binding modes between the picolinamide and benzamide series (Fig. 6). Despite the structural similarity between these two ligands, **18** was discovered to

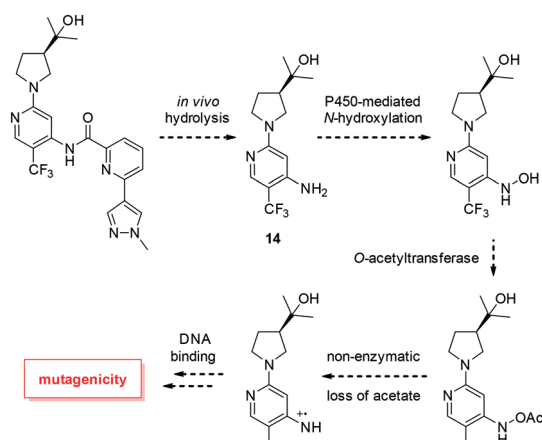


Fig. 5 Proposed mechanism for Ames mutagenicity of aromatic amine **14**. Figure adapted from Bentzien *et al.*²⁸

Table 5 Ames mutagenicity de-risking strategy: assessment of putative heteroaryl aniline metabolites in a 3-strain (TA1535, TA98, and TA100) Ames assay

	14	15	16
MCASE	Negative	Negative	Negative
QM ²⁶	Positive	Negative	Negative
3-Strain AMES	Positive	Negative	Negative

have an orthogonal binding mode relative to BMBPB-32. In compound **18**, the amide oxygen and C–H of the pyridine makes two key hydrogen bonds with backbone residues Ala1950 and Glu1948 in the kinase hinge region of LRRK2. In addition, similar to BMBPB-32, the amide N–H of **18** forms an intramolecular hydrogen bond with the pyridine nitrogen. However, compared to BMBPB-32, the pyrazole group of **18** stabilizes a conserved water network that improves hydrogen bonding with Lys1906 and catalytic Asp2017 with the methyl substituent relatively unencumbered. This suggests that different pyrazole substitution patterns could be tolerated. Toward that end, we chose to generate SAR with a variety of substituted pyrazoles. Improvements in unbound cellular potency were observed with cyclobutyl pyrazole **19** (16×), ethyl pyrazole **20** (3×), and methylcyclopropyl pyrazole **21** (53×), but without meaningful improvements in CLK2 selectivity

Table 6 Summary of 4,6-diaminopyrimidine picolinamide **17** and 4,6-diaminopyrimidine picolinamide **18**. LRRK2 IC₅₀ and Cell_u IC₅₀ values reported are *n* = 1 unless other reported (see ESI† for more information). CLK2 IC₅₀ values reported are *n* = 1

	17	18
MW, tPSA, AlogP98	421, 109, 2.05	474, 96, 3.0
LRRK2 IC ₅₀ (LBE)	4 (0.37)	17 (0.31)
Cell _u IC ₅₀ (nM)	42	21
CLK2 IC ₅₀ (nM)	255	62
CLK2/LRRK2 selectivity	64×	4×
r-PK Cl _p (mL min ⁻¹ kg ⁻¹) (Cl _{int}), MRT	3.4 (354), 4.9 h	6.7 (1271), 4.9 h
d-PK Cl _p (mL min ⁻¹ kg ⁻¹) (Cl _{int}), MRT	16.1 (756), 5.7 h	4.8 (1029), 9.4 h
1 μM rat LLC Mdr1a ER (B – A/A – B), Papp (10 ⁻⁶ cm s ⁻¹)	7.2, 35	0.94, 29
K _{p,u,u}	0.1	0.4

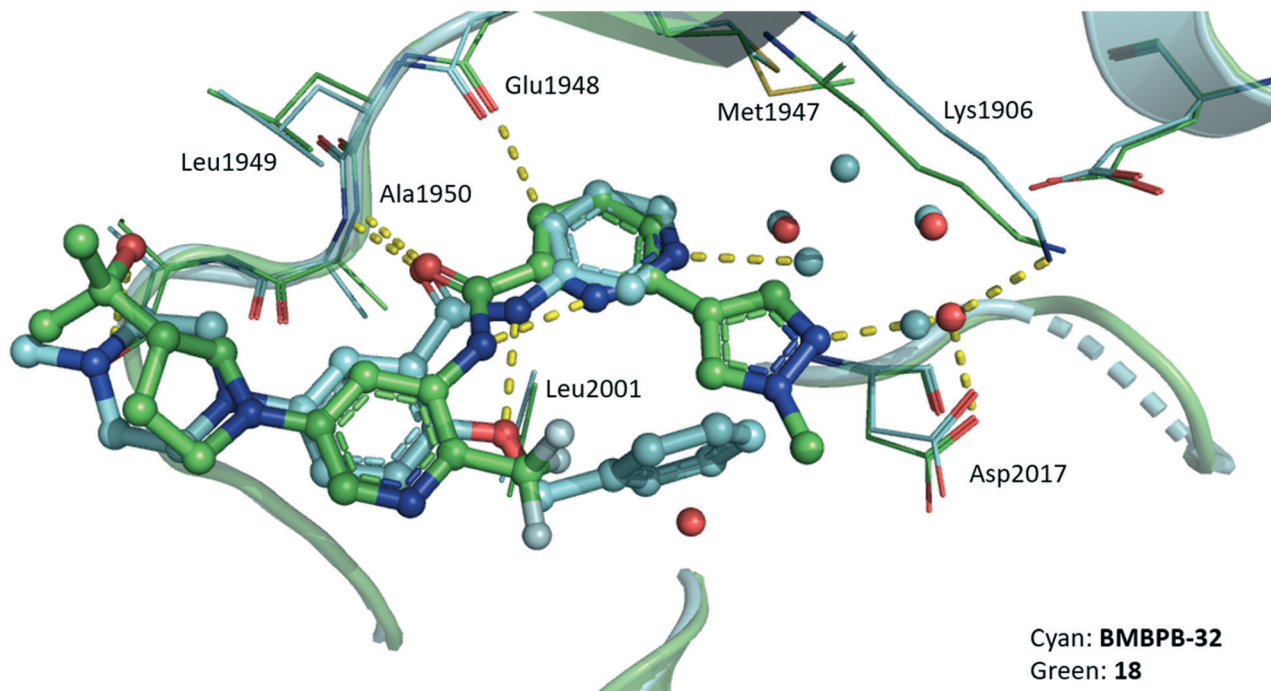
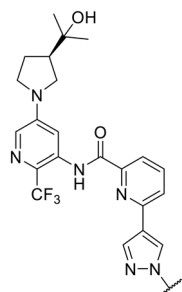
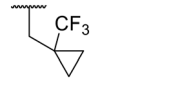


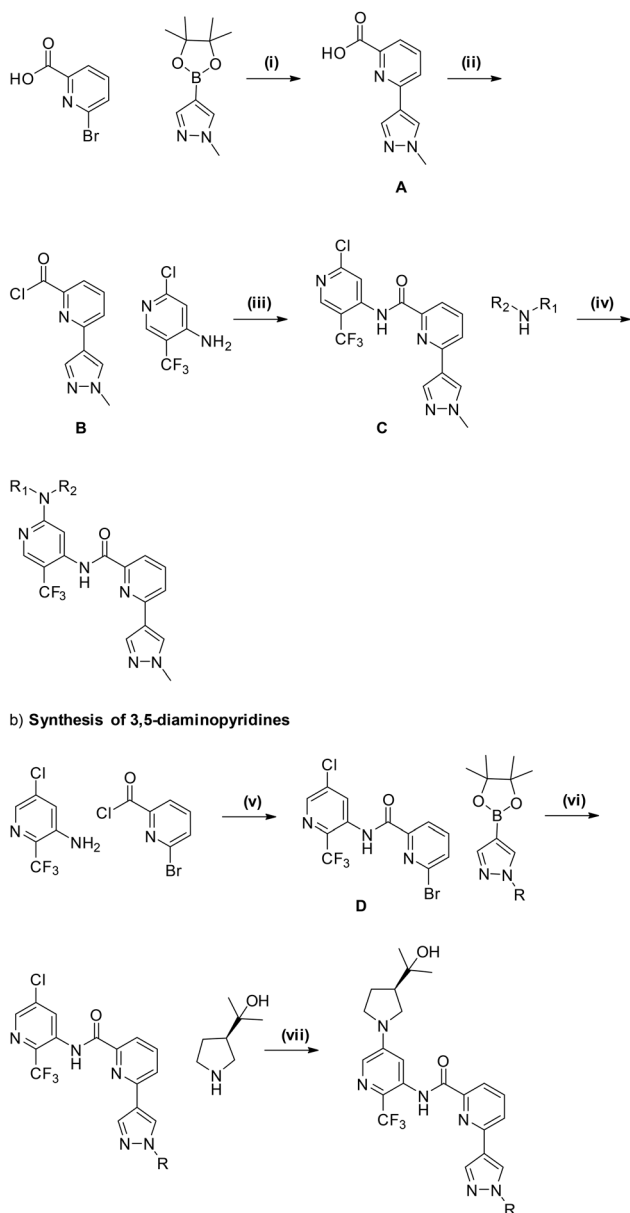
Fig. 6 Overlay of X-ray crystal structures of compound **18** (PDB code: 7MCK) and BMBPB-32 (PDB code: 5OP2).

(Table 7). The addition of a trifluoromethyl substituent afforded pyrazole **22** which had picomolar unbound cellular potency with vastly improved CLK2 selectivity (59×). Compound **22**, though, exhibited poor *in vivo* stability likely

Table 7 Catalytic lysine SAR optimization leading to the discovery of **23**. LRRK2 IC_{50} and $Cell_u$ IC_{50} values reported are $n = 1$ unless other reported (see ESI† for more information). CLK2 IC_{50} values reported are $n = 1$

	MW, tPSA, AlogP98	LRRK2 IC_{50} (LBE), $Cell_u$ IC_{50} (nM)	CLK2 IC_{50} (nM)	CLK2/LRRK2 selectivity	Rat LLC Mdr1a ER (B - A/A - B), Papp ($10^{-6} \text{ cm s}^{-1}$)	r-PK Clp $\text{mL min}^{-1} \text{ kg}^{-1}$ (Cl_{int}), MRT (h)
	514, 96, 4.0	19 (0.35), 1.3	91	5×	—	31.4 (—), 2.1 h
	488, 96, 3.4	40 (0.3), 7	30	0.8×	0.9, 19	6.7 (2883), 5.7 h
	514, 96, 3.8	8.6 (0.3), 0.4	23	3×	—	38 (78 464), 2.9 h
	582, 96, 4.6	8 (0.27), 0.3	470	59×	—	87 (—), 1.2 h
	542, 96, 4.0	10 (0.30), 0.7	442	42×	—	42 (2780), 1.7 h

a) Synthesis of 2,4-diaminopyridines



Scheme 1 Synthesis of 2,4-diaminopyridines and 3,5-diaminopyridines: (i) XPhos Pd G2, K_3PO_4 , dioxane, 80 °C, 12 h; (ii) oxalyl chloride, DMF, DCM, 25 °C, 3 h; (iii) HATU, DIEA, DMAP, DCM, 25 °C, 3 h; (iv) K_2CO_3 , MeCN, 65 °C, 12 h; (v) HATU, DIEA, DMAP, DCM, 25 °C, 3 h; (vi) $PdCl_2(tbdppf)$, K_3PO_4 , PhMe, THF, water, 70 °C, 2 h; (vii) RuPhos Pd G3, NaOtBu, dioxane, 65 °C, 12 h.

due to its enhanced lipophilicity. Trifluoroethyl pyrazole **23** maintained picomolar potency and enhanced CLK2 selectivity while demonstrating moderate *in vitro* and *in vivo* stability in rat. This resulted in an early human dose prediction of 288–520 mg BID, and prioritization for further evaluation in our ROP.

Compound **23** demonstrated weak sodium (Na^+) and calcium (Ca^{2+}) ion channel activity (Na^+ IC_{50} = 30 μ M, Ca^{2+} IC_{50} = 30 μ M), and demonstrated minimal activity against a panel of Cyp's (IC_{50} > 10 μ M). Further evaluation of kinome

selectivity resulted in only CLK4 being within 100-fold of LRRK2 potency. Compound **23** had robust pharmacokinetics in dog and rhesus monkey as demonstrated by low clearance and high MRTs across species (Table 7). Unfortunately, **23** repeatedly failed in our *in vitro* rat LLC-Mdr1a P-gp efflux transporter assay, and its pre-clinical neuro PK evaluation will be communicated in subsequent manuscript.

Synthesis of picolinamide inhibitors

The two main areas of SAR exploration for the picolinamides were in the solvent front and catalytic lysine region. We developed modular approaches allowing for the late-stage introduction of diverse moieties at each of these positions in both the 2,4-diaminopyridine series (Scheme 1a) and the 3,5-diaminopyrimidine series (Scheme 1b) starting from diverse yet simple building blocks. As an example synthesis of a 2,4-diaminopyridine, a palladium-catalyzed Suzuki coupling was used to obtain intermediate **A** which was converted to a picolinoyl chloride **B** using oxalyl chloride. Amide coupling between intermediate **B** and 2-chloro-5-(trifluoromethyl)pyridin-4-amine afforded intermediate **C**. The solvent front portion of the molecule was introduced under S_NAr conditions. As an example synthesis of a 3,5-diaminopyridine, a HATU mediated amide coupling was carried out between bromopicolinoyl chloride and 5-chloro-2-(trifluoromethyl)pyridin-3-amine to afford intermediate **D**. A selective palladium-catalyzed Suzuki coupling was carried out with several commercial and/or synthesized boronates. The amine solvent front portion of the molecule was introduced under palladium-mediated C–N coupling which afforded the desired 2,4-diaminopyridines in good yields. For additional details, the reader is directed to the ESI.†

Conclusions

In summary, the discovery of novel picolinamide derived LRRK2 inhibitors was described. This work commenced with optimization of the hinge and aryl linker moieties resulting in an advanced lead **12** that was deprioritized due to Ames mutagenicity risk. A revised strategy and ROP enabled the discovery of **18** which was low risk for Ames mutagenicity. Focused SAR optimization leveraging a CHK1-LRRK2 chimera X-ray structure to enhance potency and CLK2 selectivity led to the discovery of ethyl- CF_3 pyrazole **23** as an exquisitely potent LRRK2 inhibitor with comparable CLK2 selectivity (relative to **12**). A subsequent report detailing further optimization of this scaffold including PK/PD and pre-clinical toxicology studies will be reported in due course.

Abbreviations

ATP	Adenosine triphosphate
CNS	Central nervous system
CSF	Cerebrospinal fluid
MINK1	Misshapen-like kinase 1
IRAK4	Interleukin-1 receptor-associated kinase 4

hERG	Human ether-a-go-go
LBE	Ligand binding efficiency
MDR1	Multidrug resistance protein 1
Papp	Apparent permeability
QM	Quantum mechanical
MCASE	Multiple computer automated structure evaluation
MRT	Mean residence time
F	Bioavailability
PO	Oral administration
IC ₅₀	Concentration required to inhibit 50% of the enzyme

Author contributions

All authors have given approval to the final version of the manuscript. Specific author contributions are highlighted below. Anmol Gulati: conceptualization, methodology, formal analysis, investigation, writing – original draft. Charles S. Yeung: conceptualization, methodology, formal analysis, investigation, writing – original draft. Blair Lapointe: conceptualization, methodology, formal analysis, investigation. Solomon D. Kattar: conceptualization, methodology, formal analysis, investigation. Hakan Gunaydin: conceptualization, methodology, software, formal analysis, data curation, visualization. Jack D. Scott: conceptualization, methodology, formal analysis, investigation. Kaleen K. Childers: conceptualization, methodology, formal analysis, investigation. Joey L. Methot: conceptualization, methodology, formal analysis, investigation. Vladimir Simov: conceptualization, methodology, formal analysis, investigation. Ravi Kurukulasuriya: conceptualization, methodology, formal analysis, investigation. Barbara Pio: conceptualization, methodology, formal analysis, investigation. Greg J. Morriello: conceptualization, methodology, formal analysis, investigation. Ping Liu: conceptualization, methodology, formal analysis, supervision. Haiqun Tang: conceptualization, methodology, formal analysis, investigation. Santhosh Neelamkavil: conceptualization, supervision, project administration. Harold B. Wood: conceptualization, supervision, project administration. Vanessa L. Rada: conceptualization, methodology, formal analysis, investigation. Michael J. Ardolino: conceptualization, methodology, formal analysis, investigation. Xin Cindy Yan: conceptualization, methodology, software, formal analysis, data curation, visualization. Rachel Palte: conceptualization, methodology, formal analysis, investigation, visualization. Karin Otte: conceptualization, methodology, formal analysis, investigation, writing – review & editing. Robert Faltus: methodology, formal analysis, investigation. Janice Woodhouse: methodology, formal analysis, investigation. Laxminarayan G. Hegde: conceptualization, supervision, visualization. Paul Ciaccio: conceptualization, supervision, writing – review & editing. Ellen Minnihan: conceptualization, methodology, formal analysis, investigation. Erin F. DiMauro: supervision, writing – review & editing. Matthew J. Fell: conceptualization, supervision.

Peter H. Fuller: conceptualization, methodology, formal analysis, investigation, supervision, project administration, writing – original draft. J. Michael Ellis: conceptualization, supervision, project administration.

Conflicts of interest

There are no conflicts to declare.

Acknowledgements

We thank David J. Bennett (Merck & Co., Inc.) for proofreading this manuscript and providing constructive suggestions. We thank David A. Candito (Merck & Co., Inc.) for experimental assistance. We also thank Kelly Bleasby, Spencer Dech, Patricia Escobar, Vijay Reddy, and Bridget Ykoruk (Merck & Co., Inc.) for running several key assays described in this manuscript. We thank Evotec Protein Sciences for supply of the protein used in the structural studies presented here.

Notes and references

- 1 J. Jankovic, Motor fluctuations and dyskinesias in Parkinson's disease: Clinical manifestations, *Mov. Disord.*, 2005, **20**, S11–S16.
- 2 T. Muller and H. Russ, Levodopa, motor fluctuations and dyskinesia in Parkinson's disease, *Expert Opin. Pharmacother.*, 2006, **7**, 1715–1730.
- 3 A. B. West, D. J. Moore, S. Biskup, A. Bugayenko, W. W. Smith, C. A. Ross, V. L. Dawson and T. M. Dawson, Parkinson's disease-associated mutations in leucine-rich repeat kinase 2 augment kinase activity, *Proc. Natl. Acad. Sci. U. S. A.*, 2005, **102**, 16842–16847.
- 4 D. G. Healy, M. Falchi, S. S. O'Sullivan, V. Bonifati, A. Durr, S. Bressman, A. Brice, J. Aasly, C. P. Zabetian, S. Goldwurm, J. J. Ferreira, E. Tolosa, D. M. Kay, C. Klein, D. R. Williams, C. Marras, A. E. Lang, Z. K. Wszolek, J. Berciano, A. H. V. Schapira, T. Lynch, K. P. Bhatia, T. Gasser, A. J. Lees, N. W. Wood and International LRRK2 Consortium, Phenotype, genotype and worldwide genetic penetrance of LRRK2-associated Parkinson's disease: a case-control study, *Lancet Neurol.*, 2008, **7**, 583–590.
- 5 A. Zimprich, S. Biskup, P. Leitner, P. Lichtner, M. Farrer, S. Lincoln, J. Kachergus, M. Hulihan, R. J. Uitti, D. B. Calne, A. J. Stoessl, R. F. Pfeiffer, N. Patenge, I. C. Carbajal, P. Vieregge, F. Asmus, B. Muller-Myhok, D. W. Dickson, T. Meitinger, T. M. Strom, Z. K. Wszolek and T. Gasser, Mutations in LRRK2 cause autosomal-dominant parkinsonism with pleomorphic pathology, *Neuron*, 2004, **44**, 601–607.
- 6 W. P. Gilks, P. M. Abou-Sleiman, S. Gandhi, S. Jain, A. Singleton, A. J. Lees, K. Shaw, K. P. Bhatia, V. Bonifati, N. P. Quinn, J. Lynch, D. G. Healy, J. L. Holton, T. Revesz and N. W. Wood, A Common LRRK2 Mutation in Idiopathic Parkinsons Disease, *Lancet*, 2005, **365**(9457), 415–416.

- 7 M. Taylor and D. R. Alessi, Advances in Elucidating the Function of Leucine-Rich Repeat Protein Kinase-2 in Normal Cells and Parkinsons Disease, *Curr. Opin. Cell Biol.*, 2020, **63**, 102–113.
- 8 E. Greggio, S. Jain, A. Kingsbury, R. Bandopadhyay, P. Lewis, A. Kaganovich, M. P. V. D. Brug, A. Beilina, J. Blackinton, K. J. Thomas, R. Ahmad, D. W. Miller, S. Kesavapany, A. Singleton, A. Lees, R. J. Harvey, K. Harvey and M. R. Cookson, Kinase Activity Is Required for the Toxic Effects of Mutant LRRK2/Dardarin, *Neurobiol. Dis.*, 2006, **23**(2), 329–341.
- 9 M. Jaleel, R. J. Nichols, M. Deak, D. G. Campbell, F. Gillardon, A. Knebel and D. R. Alessi, LRRK2 Phosphorylates Moesin at Threonine-558: Characterization of How Parkinsons Disease Mutants Affect Kinase Activity, *Biochem. J.*, 2007, **405**(2), 307–317.
- 10 G. Ito, T. Okai, G. Fujino, K. Takeda, H. Ichijo, T. Katada and T. Iwatsubo, GTP Binding Is Essential to the Protein Kinase Activity of LRRK2, a Causative Gene Product for Familial Parkinsons Disease†, *Biochemistry*, 2007, **46**(5), 1380–1388.
- 11 P. Zhang, Y. Fan, H. Ru, L. Wang, V. G. Magupalli, S. S. Taylor, D. R. Alessi and H. Wu, Crystal Structure of the WD40 Domain Dimer of LRRK2, *Proc. Natl. Acad. Sci.*, 2019, **116**(5), 1579–1584.
- 12 R. Di Maio, E. K. Hoffman, E. M. Rocha, M. T. Keeney, L. H. Sanders, B. R. De Miranda, A. Zharikov, A. Van Laar, A. F. Stepan, T. A. Lanz, J. K. Kofler, E. A. Burton, D. R. Alessi, T. G. Hastings and J. T. Greenamyre, LRRK2 activation in idiopathic Parkinson's disease, *Sci. Transl. Med.*, 2018, **10**(451), eaar5429.
- 13 J. M. Hatcher, J. Zhang, H. G. Choi, G. Ito, D. R. Alessi and N. S. Gray, Discovery of a Pyrrolopyrimidine (JH-II-127), a Highly Potent, Selective, and Brain Penetrant LRRK2 Inhibitor, *ACS Med. Chem. Lett.*, 2015, **6**(5), 584–589.
- 14 R. Wallings, C. Manzoni and R. Bandopadhyay, Cellular Processes Associated with LRRK2 Function and Dysfunction, *FEBS J.*, 2015, **282**(15), 2806–2826.
- 15 H. Gunosewoyo, L. Yu, L. Munoz and M. Kassiou, Kinase Targets in CNS Drug Discovery, *Future Med. Chem.*, 2017, **9**(3), 303–331.
- 16 L. Di, H. Rong and B. Feng, Demystifying Brain Penetration in Central Nervous System Drug Discovery, *J. Med. Chem.*, 2012, **56**(1), 2–12.
- 17 T. P. Heffron, Small Molecule Kinase Inhibitors for the Treatment of Brain Cancer, *J. Med. Chem.*, 2016, **59**(22), 10030–10066.
- 18 Y. Shi and M. Mader, Brain Penetrant Kinase Inhibitors: Learning from Kinase Neuroscience Discovery, *Bioorg. Med. Chem. Lett.*, 2018, **28**(11), 1981–1991.
- 19 F. M. Moeslein, M. P. Myers and G. E. Landreth, The CLK Family Kinases, CLK1 and CLK2, Phosphorylate and Activate the Tyrosine Phosphatase, PTP-1B, *J. Biol. Chem.*, 1999, **274**(38), 26697–26704.
- 20 S. Y. Park, Y. Piao, C. Thomas, G. N. Fuller and J. F. D. Groot, Cdc2-Like Kinase 2 Is a Key Regulator of the Cell Cycle via FOXO3a/p27 in Glioblastoma, *Oncotarget*, 2016, **7**(18), 26793–26805.
- 21 H. Chen, B. K. Chan, J. Drummond, A. A. Estrada, J. Gunzner-Toste, X. Liu, Y. Liu, J. Moffat, D. Shore, Z. K. Sweeney, T. Tran, S. Wang, G. Zhao, H. Zhu and D. J. Burdick, Discovery of Selective LRRK2 Inhibitors Guided by Computational Analysis and Molecular Modeling, *J. Med. Chem.*, 2012, **55**(11), 5536–5545.
- 22 A. D. Reith, P. Bamborough, K. Jandu, D. Andreotti, L. Mensah, P. Dossang, H. G. Choi, X. Deng, J. Zhang, D. R. Alessi and N. S. Gray, GSK2578215A; A Potent and Highly Selective 2-Arylmethoxy-5-Substituent-N-Arylbenzamide LRRK2 Kinase Inhibitor, *Bioorg. Med. Chem. Lett.*, 2012, **22**(17), 5625–5629.
- 23 D. S. Williamson, G. P. Smith, P. Acheson-Dossang, S. T. Bedford, V. Chell, I.-J. Chen, J. C. A. Daechsel, Z. Daniels, L. David, P. Dokurno, M. Hentzer, M. C. Herzig, R. E. Hubbard, J. D. Moore, J. B. Murray, S. Newland, S. C. Ray, T. Shaw, A. E. Surgenor, L. Terry, K. Thirstrup, Y. Wang and K. V. Christensen, Design of Leucine-Rich Repeat Kinase 2 (LRRK2) Inhibitors Using a Crystallographic Surrogate Derived from Checkpoint Kinase 1 (CHK1), *J. Med. Chem.*, 2017, **60**(21), 8945–8962.
- 24 H. Gunaydin, M. D. Altman, J. M. Ellis, P. Fuller, S. A. Johnson, B. Lahue and B. Lapointe, Strategy for Extending Half-Life in Drug Design and Its Significance, *ACS Med. Chem. Lett.*, 2018, **9**(6), 528–533.
- 25 J. D. Scott, D. E. Demong, T. J. Greshock, K. Basu, X. Dai, J. Harris, A. Hruza, S. W. Li, S.-I. Lin, H. Liu, M. K. Macala, Z. Hu, H. Mei, H. Zhang, P. Walsh, M. Poirier, Z.-C. Shi, L. Xiao, G. Agnihotri, M. A. S. Baptista, J. Columbus, M. J. Fell, L. A. Hyde, R. Kuvelkar, Y. Lin, C. Mirescu, J. A. Morrow, Z. Yin, X. Zhang, X. Zhou, R. K. Chang, M. W. Embrey, J. M. Sanders, H. E. Tiscia, R. E. Drolet, J. T. Kern, S. M. Sur, J. J. Renger, M. T. Bilodeau, M. E. Kennedy, E. M. Parker, A. W. Stamford, R. Nargund, J. A. Mccauley and M. W. Miller, Discovery of a 3-(4-Pyrimidinyl) Indazole (MLi-2), an Orally Available and Selective Leucine-Rich Repeat Kinase 2 (LRRK2) Inhibitor That Reduces Brain Kinase Activity, *J. Med. Chem.*, 2017, **60**(7), 2983–2992.
- 26 K. M. Page, Validation of Early Human Dose Prediction: A Key Metric for Compound Progression in Drug Discovery, *Mol. Pharmaceutics*, 2016, **13**(2), 609–620.
- 27 T. S. Maurer, D. Smith, K. Beaumont and L. Di, Dose Predictions for Drug Design, *J. Med. Chem.*, 2020, **63**(12), 6423–6435.
- 28 J. Bentzien, E. R. Hickey, R. A. Kemper, M. L. Brewer, J. D. Dyekjaer, S. P. East and M. Whittaker, An in Silico Method for Predicting Ames Activities of Primary Aromatic Amines by Calculating the Stabilities of Nitrenium Ions, *J. Chem. Inf. Model.*, 2010, **50**(2), 274–297.